MediConfusion: Can you trust your AI radiologist? Probing the reliability of multimodal medical foundation models

Mohammad Shahab Sepehri
Dept. of Electrical and Computer Engineering
University of Southern California
Los Angeles, CA
sepehri@usc.edu

Zalan Fabian
Dept. of Electrical and Computer Engineering
University of Southern California
Los Angeles, CA
zfabian@usc.edu

Maryam Soltanolkotabi
Dept. of Radiology and Imaging Sciences
University of Utah
Salt Lake City, UT
maryam.soltanolkotabi@hsc.utah.edu

Mahdi Soltanolkotabi
Dept. of Electrical and Computer Engineering
University of Southern California
Los Angeles, CA
soltanol@usc.edu

Abstract

Multimodal Large Language Models (MLLMs) have tremendous potential to improve the accuracy, availability, and cost-effectiveness of healthcare by providing automated solutions or serving as aids to medical professionals. Despite promising first steps in developing medical MLLMs in the past few years, their capabilities and limitations are not well-understood. Recently, many benchmark datasets have been proposed that test the general medical knowledge of such models across a variety of medical areas. However, the systematic failure modes and vulnerabilities of such models are severely underexplored with most medical benchmarks failing to expose the shortcomings of existing models in this safety-critical domain. In this paper, we introduce MediConfusion, a challenging medical Visual Question Answering (VQA) benchmark dataset, that probes the failure modes of medical MLLMs from a vision perspective. We reveal that state-of-the-art models are easily confused by image pairs that are otherwise visually dissimilar and clearly distinct for medical experts. Strikingly, all available models (open-source or proprietary) achieve performance below random guessing on MediConfusion, raising serious concerns about the reliability of existing medical MLLMs for healthcare deployment. We also extract common patterns of model failure that may help the design of a new generation of more trustworthy and reliable MLLMs in healthcare. The evaluation code and the dataset are available at `https://github.com/AIF4S/MediConfusion`.

1 Introduction

Multimodal Large Language Models (MLLMs) have demonstrated unprecedented capabilities in a variety of multimodal tasks, including image understanding and visual reasoning, autonomous driving (Cui et al., 2024), robotics (Wang et al., 2024a) and embodied AI (Driess et al., 2023). Motivated by this success, a growing body of work (Moor et al., 2023; Li et al., 2024; Lin et al., 2023) explores the potential of MLLMs in medical applications with the hope of paving the way to more accurate, personalized and cost-effective healthcare solutions through modern generative AI.

Even though MLLMs show enormous potential in a wide range of tasks, a swath of challenges have stymied their deployment, including object hallucinations Li et al., relationship hallucinations (Wu et al., 2024), inaccurate object counting (Jain et al., 2024) and lack of spatial reasoning capabilities (Kamath et al., 2023). These shortcomings are especially worrisome in safety-critical applications, such as healthcare, where reliability is an essential requirement. In fact, recent research efforts on medical MLLMs have revealed weak anatomic knowledge (Nan et al., 2024), concerns on toxicity and patient privacy Xia et al. (2024), highly unreliable disease diagnosis Wu et al. (2023a), and the fact that even a junior doctor far outperforms the most proficient medical MLLMs across a wide spectrum of tasks Wang et al. (2024b). As model failure in the medical domain can lead to serious adverse health effects, it is of utmost importance to understand the performance and limitations of generative AI in the medical context.

A flurry of activity has emerged around probing the performance of medical MLLMs in a multitude of tasks, including visual question answering (VQA) (Ben Abacha et al., 2021), disease classification and report generation (Royer et al., 2024), and modality recognition (Wu et al., 2023b). Even though the proposed medical benchmarks offer valuable insights on model performance across a variety of anatomic regions and imaging modalities, they are focused on evaluating the medical knowledge of MLLMs across large evaluation sets, heavily biased towards common or typical scenarios. Therefore, it is unclear how well the measured performance correlates with the actual multimodal medical reasoning capabilities of these models, especially in the face of systematic but perhaps more intricate model failures underrepresented in the dataset. Therefore, developing new evaluation benchmarks that carefully test and probe the capabilities of these systems, expose their vulnerabilities, and facilitate the development of a better understanding of failure modes is vital in healthcare applications.

In this work, we introduce MediConfusion, a challenging benchmark for evaluating the failure modes of medical MLLMs from a vision perspective. We combine novel insights on the image representations of medical MLLMs with the expertise of clinical radiologists to craft a benchmark dataset that stress-tests the visual capabilities of state-of-the-art models. Our work reveals that medical MLLMs often confuse image pairs that otherwise appear very different in the image domain. Leveraging this observation, we introduce an automated pipeline to discover such pairs in the ROCO (Pelka et al., 2018) multimodal radiology dataset. Then, in collaboration with radiologists, we curate a VQA benchmark of clinically relevant multiple-choice problems designed to probe the model's ability to distinguish between such images. By design, relying solely on unimodal (language) priors cannot achieve better than random guessing accuracy on our benchmark, and therefore performance on MediConfusion directly correlates with multimodal medical reasoning and image understanding capabilities. Remarkably, we discover that both state-of-the-art medical MLLMs, as well as the most advanced proprietary models, are easily confused by the image pairs, resulting in performance *below random guessing* for all models at the time of writing this paper. What is striking about this poor performance is that for some of the models (i.e. all medical MLLMs we studied) the images and corresponding captions are part of the training data![1] Finally, we leverage our pipeline to categorize failure cases in order to guide future research toward more reliable medical AI solutions.

2   The MediConfusion Benchmark

The majority of existing multimodal foundation models leverage CLIP (Radford et al., 2021) to encode the input image (Li et al., 2024; Liu et al., 2024; Moor et al., 2023; Li et al., 2023). CLIP has been pretrained on internet-scale general domain data and, therefore, may not be suitable for the nuanced representation of medical images due to the considerable distribution shift. Thus, variants trained on large-scale medical image-text datasets have been introduced as image encoders for medical agents, including BiomedCLIP (Zhang et al., 2023b) and PMC-CLIP (Lin et al., 2023). Due to the specialized training data, these models are able to better capture the structure and semantics of medical images. However, surprisingly, we observe that the feature space of even specialized medical encoders is often not rich enough to clearly differentiate between images that are otherwise highly dissimilar. A growing body of recent work Thrush et al. (2022); Yuksekgonul et al. (2022) has shown that the contrastive pretraining objective, shared by common image encoders for MLLMs, can be optimized via shortcuts that lead to fundamental flaws in multimodal understanding. In particular,

---

[1]Given the public nature of the original dataset such images and captions are also likely part of the pretraining of proprietary models such as OpenAI's GPT-4o, Google Deep Mind's Gemini 1.5 Pro, and Anthropic's Claude 3 Opus.
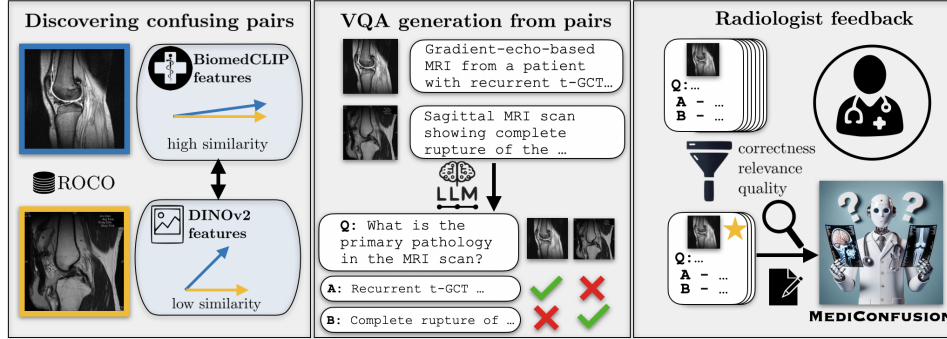
Figure 1: Overview of MediConfusion curation pipeline. First, we extract image pairs from the ROCO radiology dataset that are clearly distinct in the image domain, but may be challenging to differentiate between for multimodal models (left). Next, we use an automated pipeline leveraging LLM prompting to generate VQA from the confusing pairs and their corresponding captions (center). Finally, we incorporate radiologist feedback to filter questions for correctness, relevance and quality, and to revise the questions and answer options for improved medical language and precision (right).

training consists of aligning image features with their corresponding text features within a batch of data. Thus, if the images are clearly distinct within the batch, the task becomes easy and the model is not encouraged to learn embeddings nuanced enough for more intricate downstream tasks, such as medical reasoning. As a result, MLLMs that leverage such pretrained encoders suffer from impaired image understanding and visual reasoning (Tong et al., 2024a,b), casting serious doubt on the reliability of such models in critical medical diagnosis. Therefore, designing challenging benchmarks that stress-test the visual capabilities of medical MLLM is of utmost importance for gaining a better understanding of the limitations of existing models.

In this work, we introduce the MediConfusion Benchmark, a challenging multiple choice medical visual question answering benchmark designed to probe the reasoning capabilities of medical MLLMs. The overview of our curation pipeline is summarized in Figure 1. First, we extract image pairs that are visually clearly different, but MLLMs will likely confuse them due to their similar features in embedding space. Next, based on the captions corresponding to each of the images in the confusing pairs, we generate a large pool of multiple choice problems via LLM prompting. Finally, each question in the LLM-generated pool is scrutinized and revised by an expert radiologist before being added to MediConfusion. We evaluate a range of state-of-the-art medical and general domain MLLMs and demonstrate that even flagship proprietary models have performance worse than random guessing.

Discovering confusing pairs– We find confusing image pairs in ROCO (Pelka et al., 2018), a multimodal dataset of $\approx 80k$ radiology images and their corresponding captions extracted from PMC-OA (Lin et al., 2023) (Figure 1, left). Inspired by Tong et al. (2024b), we seek out pairs with clear visual differences, but high similarity in the feature space of the medical MLLMs. This implies that at least one of the images in the pair is compressed ambiguously, and thus, it is likely that relevant visual information is lost in the encoding. In particular, we base our selection criteria on BiomedCLIP's embedding space, as this model has been specifically trained on medical image-text data, and thus it has a more refined feature space for medical images than a general-domain encoder, such as CLIP. Simply put, a radiology image pair that confuses BiomedCLIP, will likely confuse CLIP as well. Moreover, BiomedCLIP has been pretrained on the largest dataset of medical image-caption data among publicly available CLIP-style biomedical vision-language models. We measure visual differences between images in the feature space of DINOv2, a state-of-the-art vision-only foundation model with robust image representations that capture visual details. We randomly sample pairs of images and evaluate their similarity in BiomedCLIP (sim_{med}) and DINOv2 (sim_{gen}) feature spaces. We consider them a confusing pair if $sim_{med} \geq 0.9$ and $sim_{gen} \leq 0.75$ hold at the same time. The gap $|sim_{med} - sim_{gen}|$ can be increased further in order to obtain more difficult pairs; however, we find that our setting is already challenging enough for most contemporary models. We depict sample pairs uncovered by our technique in Appendix C.

VQA generation– Given a pool of candidate confusing pairs, we generate multiple choice medical VQA problems that probe the MLLM's ability to effectively differentiate between the images in the pair (Figure 1, center). First, we filter the candidate pool by removing images with short captions
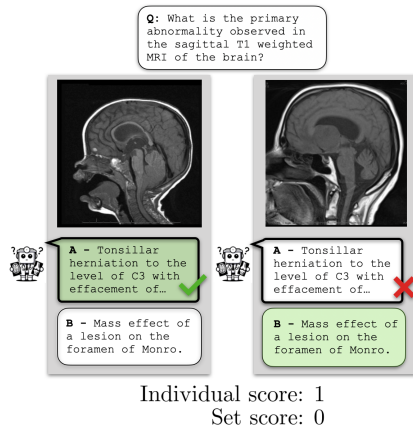
Figure 2: A sample question pair from MediConfusion. A confusing pair shares the same question and corresponding answer options, but the correct answer is different for the two. The model receives a *set score* of 1 only if it correctly answers both questions in the confusing pair. *Individual score* is evaluated separately for each image.
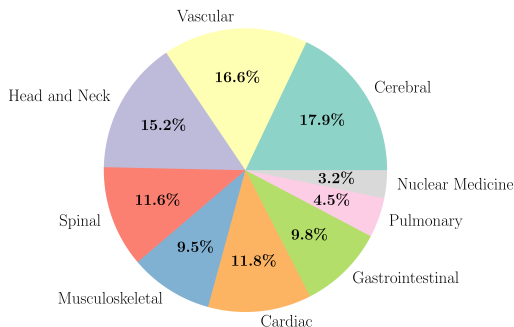

Figure 3: Distribution of question categories in MediConfusion. We assign a category to the question based on the category of the corresponding image in the VQA. A single image can belong to multiple categories at the same time.

(< 100 characters) that likely contain insufficient detail about the image. Next, we pass the pair of captions to an LLM (GPT-4) and prompt the model to *generate a question to which the answer is different for the two images* and to provide the two answer options. Thus, we create two VQA problems for each pair that share the same question and answer options, however the correct answer is different for the two images (Figure 2). Therefore, if the medical MLLM is unable to differentiate between the input images, it would only be able to answer at most one of the pair of VQA problems correctly, but not both. As a result, our benchmark by construction cannot be solved to higher than 50% accuracy by relying solely on language prior. In particular, we only credit a *set score* to the model on a particular question pair, if the question has been answered correctly for both images. On the other hand, as a less strict metric an *individual score* is awarded to the model for each correct answer, irrespective of correctness on the other image in the pair. Furthermore, in order to categorize questions in the VQA, we prompt the LLM to assign the most relevant medical area to each of the questions based on the corresponding image's PMC caption. We leverage these categories to break down the performance of existing medical MLLMs across the various categories. We include all prompts used in VQA generation in Appendix A.

Data filtering and revision via radiologist feedback– As we generate the questions/answer choices using an LLM, various issues may arise such as factual errors and inconsistencies in quality, format, or language. To ensure the curation of a reliable benchmark dataset, oversight and feedback from a radiology expert are crucial. A radiologist evaluated each of the automatically generated VQA problems focusing on three aspects.

Correctness: the question has to be valid with respect to both of the images, the problems need to be solvable by looking at the individual images alone, and the corresponding answers have to be correct.

Relevance: the question has to be relevant to clinical practice or medical research.

Language: the problem has to use proper medical terminology and precise language.

Based on these guidelines, the radiologist assigned a quality score to each question, on a scale $1-10$. Higher scores correspond to better problems, and a score of 1 is assigned if correctness is violated in any form (e.g., irrelevant question, incorrect answer). We add a VQA pair to MediConfusion only if the quality score is at least 5 for both individual problems in the pair. Moreover, the expert verified the medical categories assigned by the LLM to each of the images and revised the question and answer options to improve language quality and precision. This step is crucial in eliminating model artifacts that originate in LLM-generated text inputs.

The resulting benchmark is well-rounded, with questions touching upon 9 areas (see Figure 3): *cerebral*, *spinal*, *cardiac*, *gastrointestinal*, *musculoskeletal*, *vascular*, *pulmonary*, *head and neck*, and *nuclear medicine* with 352 questions in total. Figure 3 depicts the distribution of question categories.

3 Experiments

3.1 Evaluation

We evaluate models on MediConfusion based on two notions of accuracy. *Set accuracy* is the portion of correct confusing pairs, where we only consider a pair correct if the model has answered the question correctly for both images in the pair. *Individual accuracy* is the standard notion of accuracy, that is, the portion of correct answers over all questions. An example is depicted in Figure 2. Furthermore, we report *confusion score*, which indicates the portion of pairs where the model has chosen the same answer for both images in the pair, out of all pairs (we exclude pairs where the model generated invalid answers or failed to answer). A high confusion score signifies that the model prediction is overwhelmingly invariant to the specific input image within a pair, and thus, it is confused by the images.

Extracting the knowledge from MLLMs for VQA benchmarking is often challenging due to sensitivity to the specific prompt format and phrasing, strong reliance on language bias and other factors. For instance, instruction tuned models can be directly prompted to answer a multiple choice question with the correct letter option, whereas models without instruction tuning often fail to do so. Therefore, in order to provide a fair comparison, we use a range of evaluation techniques to assess performance.

Prefix-based score (PS) – Following Xu et al. (2023), we compute the normalized likelihood of image-question-answer triplets for each answer option, and pick the option with the highest likelihood as the answer. In other words, we select the answer option that the model assigns the highest probability to, given the image and question. To compute the prefix-based score, we concatenate the medical question and the answer sentence directly, stripping the multiple choice question style (e.g., removing "Choose the letter of the correct answer.") and option indicators (e.g., removing "Option A: ...") in order to ensure that models that have not been specifically trained on multiple choice question answering can also consistently provide valid answers.

Multiple choice prompting (MC) – We directly prompt the model to answer the multiple choice question with the letter of the correct option. As the output formats may vary (e.g., "A" vs. "The answer is A."), we parse the outputs and attempt to match it to one of the answer options.

Free-form evaluation (FF) – We prompt the model to answer the question without providing the answer options or requiring any specific output format. Then, we attempt to match the model output to one of the options using an LLM. In particular, we prompt GPT-4 to score how well the generated output matches each of the options, and we pick the answer option with the highest score. We include the specific evaluation prompt in Appendix A.

Greedy decoding (GD)– Similar to multiple choice prompting, we directly prompt the model to answer the problem with the letter of the correct option, then we pick the option with the highest assigned next-token probability. Greedy decoding evaluation is a special case of prefix-based scoring, where the answer options consist of a single letter.

PS and FF evaluations are suitable for models that are not instruction tuned or have not been trained to understand the multiple choice QA format. On the other hand, MC and GD are simpler to evaluate, however these techniques may fail to correctly measure the knowledge of MLLMs unable to understand and follow the multiple choice format. Overall, we represent the performance of each model by their best performance across all evaluation techniques. As we observe, proprietary models can consistently pick an answer option for multiple choice questions; for these models, we only provide MC results. Moreover, output logits necessary for PS and GD evaluation are not available for proprietary models.

We evaluate a representative set of 12 models, 3 of which are medical MLLMs (LLaVA-Med (Li et al., 2024), Med-Flamingo (Moor et al., 2023), RadFM (Wu et al., 2023b)), 3 are flagship proprietary models (GPT-4o, Claude 3 Opus, Gemini 1.5 Pro) and 6 open-source general-domain MLLMs (LLaVA-7B v1.6 (Liu et al., 2024), BLIP-2 (Li et al., 2023), InstructBLIP (Dai et al., 2023), Llama 3.2 90B, and Molmo 72B and 7B). We set generation parameters according to the corresponding

Method	Set acc. (%)				Indiv. acc.(%)				Confusion (%)				Best	
	MC	GD	FF	PS	MC	GD	FF	PS	MC	GD	FF	PS	Set acc.	Indiv. acc.
Llama 3.2	<u>15.34</u>	14.77	2.84	9.66	54.55	<u>55.97</u>	21.02	50.85	78.41	82.39	75.61	82.39	15.34	55.97
Molmo 72B	<u>6.82</u>	<u>6.82</u>	1.7	3.98	49.72	<u>52.56</u>	18.75	50.57	85.80	91.48	90.91	93.18	6.82	52.96
Molmo 7B	<u>9.66</u>	0.57	0.57	5.11	<u>52.84</u>	49.72	14.77	51.42	86.21	98.3	83.33	92.61	9.66	52.84
LLaVA	8.52	<u>9.09</u>	1.70	1.14	50.57	<u>51.70</u>	15.06	49.72	85.47	85.80	76.00	97.16	9.09	51.70
BLIP-2	0.57	<u>6.82</u>	1.70	3.98	22.16	50.28	11.65	<u>51.42</u>	92.19	86.93	86.67	94.89	6.82	51.42
InstructBLIP	<u>12.50</u>	7.95	2.84	3.41	51.99	<u>53.12</u>	19.60	50.57	80.35	90.34	87.23	94.32	12.50	53.12
LLaVA-Med	0.00	0.00	<u>1.14</u>	<u>1.14</u>	23.58	<u>49.72</u>	18.75	<u>49.72</u>	100.00	99.43	95.92	97.16	1.14	49.72
RadFM	0.57	1.14	0.57	<u>5.68</u>	35.90	<u>50.28</u>	16.19	48.58	97.54	98.30	95.12	85.80	5.68	50.28
Med-Flamingo	1.14	2.27	0.57	<u>4.55</u>	47.73	50.00	17.05	<u>51.99</u>	98.75	95.45	94.89	98.30	4.55	51.99
GPT-4o	18.75	-	-	-	56.25	-	-	-	75.00	-	-	-	18.75	**56.25**
Claude 3 Opus	8.52	-	-	-	50.85	-	-	-	84.09	-	-	-	8.52	50.85
Gemini 1.5 Pro	19.89	-	-	-	51.14	-	-	-	58.52	-	-	- -	19.89	51.14
Random guessing													**25.00**	50.00

Table 1: Experimental results on MediConfusion. Evaluation techniques: PS - prefix-based scoring, MC - multiple choice prompting, FF - free-form evaluation, GD - greedy decoding evaluation. We <u>underscore</u> the best accuracy for each method across evaluation techniques and report the overall best in **bold**.

code release and recommended settings and use few-shot prompting for Med-Flamingo (more details in Appendix B).

3.2 Results

We summarize the performance of MLLMs on MediConfusion in Table 1. Alarmingly, all MLLMs perform below random guessing in terms of set accuracy, corroborating our hypothesis that models struggle to differentiate in fine enough detail between the extracted image pairs necessary for accurate medical reasoning. This observation is further supported by the markedly high (often above 90%) confusion scores indicating that models tend to select the same answer for both images within a confusing pair. Even RadFM, a model that does not leverage a CLIP-style image encoder, is confused on our benchmark (82.39% confusion score) with performance well below random guessing. As most likely proprietary models leverage visual encoders other than CLIP as well, the overall poor performance and extremely high confusion scores suggest that the exposed vulnerability is more general and not solely rooted in the specific ambiguities of CLIP encoding.

An interesting outlier is Gemini 1.5, which has been the least confused (approx. 60%) on the dataset; however, its accuracy is still close to random guessing. This may suggest that the model's visual representations are rich enough to meaningfully distinguish between images; however, the medical knowledge or necessary reasoning skills are lacking to correctly answer the questions.

Furthermore, perhaps surprisingly, medical MLLMs did not outperform other methods, which indicates that the shortcomings cannot be addressed exclusively by domain-specific training. These results are especially surprising, as the image-caption pairs used to generate MediConfusion are part of PMC-OA, which is included in the pre-training set of all 3 medical MLLMs in our experiments. We also note that given the public nature of PMC-OA these image-caption pairs are likely included in the training set of proprietary models as well. Finally, we do see some performance gap between open-source and proprietary models, with GPT-4o achieving the highest individual accuracy, however, barely surpassing that of random guessing (56.25% vs. 50%) with set accuracy still well below random guessing.

We further break down the results based on the category of the question in order to identify if specific areas have been more/less challenging to the models. We summarize our findings in Appendix C. Even though the overall results across all categories are close to random guessing performance, proprietary models demonstrate slightly better accuracies on questions related to cerebral and vascular images. In particular, GPT-4o achieves 34.25% and 67.12% set and individual accuracy correspondingly on vascular images, an overall best across all models and categories

4 Discussion

4.1 Identifying Patterns in Confusing Pairs

Our experiments have demonstrated that state-of-the-art MLLMs are easily confused by radiology image pairs that exhibit major differences obvious to human experts. The first step towards improving the reliability of such models is to identify and categorize common cases where medical MLLMs tend to break down. We leverage an expert-in-the-loop pipeline to extract failure modes from MediConfusion via a combination of LLM prompting and radiologist supervision. In particular, we pass the VQA problems from MediConfusion to GPT-4, where we replace the images with their corresponding captions from ROCO. We prompt the model to summarize the key differences between images in a pair that the questions are designed to test (details in Appendix A). The LLM identifies patterns in the extracted differences and distills them into a set of categories that the radiologist corrects and refines based on the dataset. As a result, we identify the following common patterns that have confused the models:

Pattern 1: Normal/variant anatomy vs. pathology– Models often struggle with differentiating between normal/variant anatomy and pathological structures. For instance, the model often confuses malalignment with normal alignment (e.g., atlantoaxial dislocation vs. normal atlantoaxial interval) or differentiating pituitary region masses (suprasellar vs. parasellar vs. intrasellar) or various anatomical regions of the spine (cervical vs. thoracic vs. lumbar).

Pattern 2: Lesion signal characteristics– Models fail to correctly identify regions of high signal intensity and their significance, particularly on T2-weighted sequences. This failure is especially of clinical significance in differentiating solid vs. cystic entities.

Pattern 3: Vascular conditions– Identifying aneurysms and differentiating them from normal vascular structures or other abnormalities like vascular malformations seems to be challenging for MLLMs. Furthermore, there is often confusion between total occlusions and partial stenosis in coronary arteries.

Pattern 4: Medical devices– Models often fail to detect the presence of stents and have difficulties distinguishing between various types of stents. Identifying the presence or absence of guidewires in images of interventional procedures tends to also be challenging for MLLMs.

Most of the above shortcomings can be, to some degree, traced back to known, common failure modes (Tong et al., 2024b) of visual reasoning in MLLMs in the general domain.

Detecting presence (or absence) of specific features: Correct reasoning over medical VQA problems strongly relies on detecting the presence (or absence) of particular features or objects relevant to the question. MLLMs are known to suffer from object hallucinations (Li et al.) rooted in parts in flawed image encoding, statistical biases and strong reliance on language priors (Leng et al., 2024). We can see this specific weakness reflected in Patterns 3 and 4 directly.

Understanding state and condition: In medical VQA, it is crucially important for the model to understand the difference between "normal" and "abnormal" structures. MLLMs have difficulties identifying the state and condition of objects in the general domain, such as whether the ground is wet or if a flag is blowing in the air (Tong et al., 2024b). These challenges may be amplified in the more nuanced medical setting, which we observe in Patterns 1 and 3 especially.

Positional and relational context: Answering medical VQA problems often necessitate a careful understanding of the spatial relationships of various anatomical features and their specific location. Recent research has uncovered serious limitations in the spatial reasoning capabilities of MLLMs (Kamath et al., 2023), some even failing to distinguish left from right. This pervasive weakness in spatial reasoning may translate to failures in medical VQA seen in Pattern 1.

Color and appearance: Recent work has shown that MLLMs can confuse colors and their intensity (bright/dark) (Tong et al., 2024b), which may cause challenges in identifying signal characteristics in radiology images (high/low intensity) reflected in Pattern 2.

4.2 Visual Prompts in MediConfusion

Free-form visual prompts are intuitive annotations in the input image, such as a red bounding box or an arrow, aimed at highlighting a specific point or area within the image. It is natural to ask

whether well-placed visual prompts in medical images, annotated by a doctor, can potentially guide the attention of MLLMs to important areas in the image and thus help provide accurate answers. Such a capability would greatly facilitate human-machine collaboration in healthcare and provide more reliable AI-assisted diagnosis. In the general domain, research has shown that MLLMs typically are unable to efficiently interpret visual prompts without incorporating such task specifically into the training procedure (Cai et al., 2024).

We find that some images in MediConfusion include such visual prompts, typically in the form of arrows pointing at the abnormality, and in a specific case the correct answer is written in the image along with the prompt (Figure 4 in the Appendix). We observe that only proprietary models, as well as LLaVA v1.6 and BLIP-2, have been able to provide consistently correct answers for this particular image, and none of the medical MLLMs. We hypothesize that the success of proprietary models and LLaVA v1.6 can be attributed to their OCR (optical character recognition) capabilities, which are missing from medical MLLMs. In examples where only the visual prompt (e.g., an arrow pointing at the abnormality/region of interest) is included, we don't observe a similar trend. We believe that understanding and improving the visual prompting capabilities of medical MLLMs is a promising direction for future research.

5 Related Work

Multimodal Large Language Models (MLLMs)– Beyond the general domain, MLLMs are especially promising in automating costly medical tasks, such as analyzing radiology images, generating medical reports or acting as medical conversational agents to provide healthcare advice. There has been substantial research recently to develop medical MLLMs, most often by adapting popular general domain architectures to medical data. Med-Flamingo (Moor et al., 2023) pretrains Flamingo on interleaved image-text medical data sourced from publications and textbooks, unlocking few-shot medical VQA capabilities. Authors of LLaVA-Med (Li et al., 2024) focus on rapid adaptation to the medical domain by fine-tuning LLaVA on filtered image-text pairs from PMC-15M (Zhang et al., 2023a). Authors in Zhang et al. (2023c) generate a large-scale medical VQA dataset from PMC-OA (Lin et al., 2023) which is subsequently used to train MedVInT, a state-of-the-art medical MLLM. Moreover, authors in Wu et al. (2023b) propose a multimodal foundation model for radiology, aligning natural language with 2D and 3D radiology images.

Encoding visual information in MLLMs– The prevailing approach to incorporate visual information in MLLM training is to leverage contrastive language-image pretrained models as frozen image encoders. CLIP (Radford et al., 2021), and its variants (Cherti et al., 2023), are trained on internet-scale image-text data, and thus its representations are readily aligned with natural language, and can be effectively combined with language models. The frozen representations are typically adapted to the feature space of the language model using MLP heads (Liu et al., 2024), Q-Former (Li et al., 2022), cross-attention (Alayrac et al., 2022) or other mechanisms. The image encoder acts as the "eye" of the MLLM as it directly determines what visual information will enter the model. In fact, imperfect compression of relevant visual information is a dominant issue with contemporary MLLMs, resulting in object hallucinations (Li et al.; Gunjal et al., 2024), fundamental errors in spatial reasoning (Kamath et al., 2023), and inability to understand inter-object relationships (Wu et al., 2024).

As the distribution of general 'internet data' and medical image-text data is markedly different, CLIP may be unable to capture the intricate structure of medical images with fidelity sufficient for reliable performance. Researchers have proposed CLIP-like models pretrained on large-scale medical data better suited as image encoders for medical MLLMs. LLaVA-Med leverages BiomedCLIP (Zhang et al., 2023b), a foundation model designed for biomedical image-text processing that has been pretrained on PMC-15M. MedVInT uses PMC-CLIP (Lin et al., 2023), a CLIP-style model pretrained on PMC-OA with $1.6M$ medical image-caption pairs. The limitations of image encoders in medical MLLMs have attracted less attention than in the general domain, which is especially troubling due to the safety-critical nature of healthcare applications. Thus, the lack of in-depth understanding of the shortcomings and possible failure modes of the image encoder in the medical MLLM pipeline is an exceedingly pressing concern.

Medical VQA benchmarks– With the recent rapid advances in developing medical MLLMs, there has been substantial effort in quantifying their performance in a wide range of tasks within the medical domain. VQA-Rad (Lau et al., 2018), SLAKE (Liu et al., 2021), Path-VQA (He et al., 2020) and VQA-Med (Ben Abacha et al., 2021) are widely-used to benchmark the performance

of MLLMs in medical VQA. Due to their small size and limited scope, there has been a push for more comprehensive and diverse evaluation datasets. OmniMedVQA (Hu et al., 2024) introduces the largest medical VQA dataset to date, encompassing 12 data modalities and 20 anatomical regions with a total of more than $100k$ images. Authors of Asclepius (Wang et al., 2024b) focus on eliminating data leakage present in other benchmarks and providing human evaluations. GMAI-MMBench (Chen et al., 2024) incorporates problems probing the performance of MLLMs at various perceptual granularities, and targets a well-categorized data structure for ease of preparing customized evaluations. Other benchmarks extend the evaluation task beyond VQA to provide a more comprehensive view of model performance. MultiMedEval (Royer et al., 2024) builds a uniform and fair benchmarking framework for multiple tasks including report generation and classification. RadBench (Wu et al., 2023b) focuses on radiology with associated tasks such as modality recognition and disease diagnosis. CARES (Xia et al., 2024) aims to provide a more holistic view of model performance by focusing on aspects such as fairness, privacy and safety (toxicity) of MLLMs as well as factual correctness (trustfulness).

All of these datasets are aimed at probing the medical knowledge of MLLMs and quantifying their average performance on a wide variety of tasks, modalities and anatomic regions. However, none of these benchmarks are specifically designed to probe the reliability, fundamental limitations and failure modes in the medical domain, all critical aspects in healthcare applications.

Perhaps the closest work in spirit to ours is RadVUQA (Nan et al., 2024), where authors call attention to the critical deficiencies of existing medical MLLMs, revealing a large gap between state-of-the-art MLLMs and clinicians. Their dataset focuses on more fundamental visual question answering and understanding, such as spatial reasoning, anatomic understanding and quantitative reasoning on medical images. However, we go a step further and design a benchmark that stress-tests the visual capabilities of MLLMs by curating questions expected to be challenging for the image processing pipeline of state-of-the-art models.

Related to our work, Tong et al. (2024b) has investigated the failure modes of MLLMs originating in ambiguous vision encoding in the general domain. Their study is based on finding CLIP-blind pairs, images that have high similarity in CLIP embedding space, but otherwise have dissimilar low-level image features. However, their methodology is not directly applicable in the medical domain for two reasons. First, CLIP has been pretrained on general domain data and thus it is unable to capture the intricate structure of medical images. Second, their methodology relies on human annotators to describe the difference between a large number of image pairs, which is prohibitively costly in our scenario, as only radiologists are qualified to provide such annotations in the medical setting.

6 Conclusion

In this paper, we introduce MediConfusion, a challenging medical VQA benchmark designed to probe the limitations of multimodal reasoning in medical MLLMs. In particular, we discover radiology image pairs that, due to ambiguities originating in image encoding, confuse contemporary models despite being dissimilar in the image domain. We leverage an automated pipeline along with the expertise of radiologists to create a dataset of VQA problems that tests the ability of MLLMs to effectively distinguish and answer clinically relevant questions about such confusing pairs. Our benchmark, by construction, cannot be solved by leveraging unimodal priors, and thus, it directly probes multimodal capabilities. We find that existing models achieve performance no better than random guessing on MediConfusion, as models tend to select the same answer option for both images in the pair, raising serious concerns about the reliability of existing MLLMs in a medical setting. In order to guide future research in addressing the limitations of current MLLMs, we identify common failure patterns where models often break and relate them to known limitations in the general domain. We hope that our work sparks further research efforts to improve the reliability of AI for healthcare applications.

Acknowledgements

References

Alayrac, J.-B., Donahue, J., Luc, P., Miech, A., Barr, I., Hasson, Y., Lenc, K., Mensch, A., Millican, K., Reynolds, M., et al. Flamingo: a visual language model for few-shot learning. *Advances in neural information processing systems*, 35:23716–23736, 2022.

Ben Abacha, A., Sarrouti, M., Demner-Fushman, D., Hasan, S. A., and Müller, H. Overview of the vqa-med task at imageclef 2021: Visual question answering and generation in the medical domain. In *Proceedings of the CLEF 2021 Conference and Labs of the Evaluation Forum-working notes*. 21-24 September 2021, 2021.

Cai, M., Liu, H., Mustikovela, S. K., Meyer, G. P., Chai, Y., Park, D., and Lee, Y. J. Vip-llava: Making large multimodal models understand arbitrary visual prompts. In *Proceedings of the IEEE/CVF Conference on Computer Vision and Pattern Recognition*, pp. 12914–12923, 2024.

Chen, P., Ye, J., Wang, G., Li, Y., Deng, Z., Li, W., Li, T., Duan, H., Huang, Z., Su, Y., et al. Gmai-mmbench: A comprehensive multimodal evaluation benchmark towards general medical ai. *arXiv preprint arXiv:2408.03361*, 2024.

Cherti, M., Beaumont, R., Wightman, R., Wortsman, M., Ilharco, G., Gordon, C., Schuhmann, C., Schmidt, L., and Jitsev, J. Reproducible scaling laws for contrastive language-image learning. In *Proceedings of the IEEE/CVF Conference on Computer Vision and Pattern Recognition*, pp. 2818–2829, 2023.

Cui, C., Ma, Y., Cao, X., Ye, W., Zhou, Y., Liang, K., Chen, J., Lu, J., Yang, Z., Liao, K.-D., et al. A survey on multimodal large language models for autonomous driving. In *Proceedings of the IEEE/CVF Winter Conference on Applications of Computer Vision*, pp. 958–979, 2024.

Dai, W., Li, J., LI, D., Tiong, A., Zhao, J., Wang, W., Li, B., Fung, P. N., and Hoi, S. InstructBLIP: Towards General-purpose Vision-Language Models with Instruction Tuning. In Oh, A., Naumann, T., Globerson, A., Saenko, K., Hardt, M., and Levine, S. (eds.), *Advances in Neural Information Processing Systems*, volume 36, pp. 49250–49267. Curran Associates, Inc., 2023. URL https://proceedings.neurips.cc/paper_files/paper/2023/file/9a6a435e75419a836fe47ab6793623e6-Paper-Conference.pdf.

Driess, D., Xia, F., Sajjadi, M. S., Lynch, C., Chowdhery, A., Ichter, B., Wahid, A., Tompson, J., Vuong, Q., Yu, T., et al. Palm-e: An embodied multimodal language model. *arXiv preprint arXiv:2303.03378*, 2023.

Gunjal, A., Yin, J., and Bas, E. Detecting and preventing hallucinations in large vision language models. In *Proceedings of the AAAI Conference on Artificial Intelligence*, volume 38, pp. 18135–18143, 2024.

He, X., Zhang, Y., Mou, L., Xing, E., and Xie, P. Pathvqa: 30000+ questions for medical visual question answering. *arXiv preprint arXiv:2003.10286*, 2020.

Hu, Y., Li, T., Lu, Q., Shao, W., He, J., Qiao, Y., and Luo, P. Omnimedvqa: A new large-scale comprehensive evaluation benchmark for medical lvlm. In *Proceedings of the IEEE/CVF Conference on Computer Vision and Pattern Recognition*, pp. 22170–22183, 2024.

Jain, J., Yang, J., and Shi, H. Vcoder: Versatile vision encoders for multimodal large language models. In *Proceedings of the IEEE/CVF Conference on Computer Vision and Pattern Recognition*, pp. 27992–28002, 2024.

Kamath, A., Hessel, J., and Chang, K.-W. What's "up" with vision-language models? investigating their struggle with spatial reasoning. In *Proceedings of the 2023 Conference on Empirical Methods in Natural Language Processing*, pp. 9161–9175, 2023.

Lau, J. J., Gayen, S., Ben Abacha, A., and Demner-Fushman, D. A dataset of clinically generated visual questions and answers about radiology images. *Scientific data*, 5(1):1–10, 2018.

Leng, S., Zhang, H., Chen, G., Li, X., Lu, S., Miao, C., and Bing, L. Mitigating object hallucinations in large vision-language models through visual contrastive decoding. In *Proceedings of the IEEE/CVF Conference on Computer Vision and Pattern Recognition*, pp. 13872–13882, 2024.

Li, C., Wong, C., Zhang, S., Usuyama, N., Liu, H., Yang, J., Naumann, T., Poon, H., and Gao, J. Llava-med: Training a large language-and-vision assistant for biomedicine in one day. *Advances in Neural Information Processing Systems*, 36, 2024.

Li, J., Li, D., Xiong, C., and Hoi, S. Blip: Bootstrapping language-image pre-training for unified vision-language understanding and generation. In *International conference on machine learning*, pp. 12888–12900. PMLR, 2022.

Li, J., Li, D., Savarese, S., and Hoi, S. Blip-2: Bootstrapping language-image pre-training with frozen image encoders and large language models. In *International conference on machine learning*, pp. 19730–19742. PMLR, 2023.

Li, Y., Du, Y., Zhou, K., Wang, J., Zhao, X., and Wen, J.-R. Evaluating object hallucination in large vision-language models. In *The 2023 Conference on Empirical Methods in Natural Language Processing*.

Lin, W., Zhao, Z., Zhang, X., Wu, C., Zhang, Y., Wang, Y., and Xie, W. Pmc-clip: Contrastive language-image pre-training using biomedical documents. In *International Conference on Medical Image Computing and Computer-Assisted Intervention*, pp. 525–536. Springer, 2023.

Liu, B., Zhan, L.-M., Xu, L., Ma, L., Yang, Y., and Wu, X.-M. Slake: A semantically-labeled knowledge-enhanced dataset for medical visual question answering. In *2021 IEEE 18th International Symposium on Biomedical Imaging (ISBI)*, pp. 1650–1654. IEEE, 2021.

Liu, H., Li, C., Wu, Q., and Lee, Y. J. Visual instruction tuning. *Advances in neural information processing systems*, 36, 2024.

Moor, M., Huang, Q., Wu, S., Yasunaga, M., Dalmia, Y., Leskovec, J., Zakka, C., Reis, E. P., and Rajpurkar, P. Med-flamingo: a multimodal medical few-shot learner. In *Machine Learning for Health (ML4H)*, pp. 353–367. PMLR, 2023.

Nan, Y., Zhou, H., Xing, X., and Yang, G. Beyond the hype: A dispassionate look at vision-language models in medical scenario. *arXiv preprint arXiv:2408.08704*, 2024.

Pelka, O., Koitka, S., Rückert, J., Nensa, F., and Friedrich, C. M. Radiology objects in context (roco): a multimodal image dataset. In *Intravascular Imaging and Computer Assisted Stenting and Large-Scale Annotation of Biomedical Data and Expert Label Synthesis: 7th Joint International Workshop, CVII-STENT 2018 and Third International Workshop, LABELS 2018, Held in Conjunction with MICCAI 2018, Granada, Spain, September 16, 2018, Proceedings 3*, pp. 180–189. Springer, 2018.

Radford, A., Kim, J. W., Hallacy, C., Ramesh, A., Goh, G., Agarwal, S., Sastry, G., Askell, A., Mishkin, P., Clark, J., et al. Learning transferable visual models from natural language supervision. In *International conference on machine learning*, pp. 8748–8763. PMLR, 2021.

Royer, C., Menze, B., and Sekuboyina, A. Multimedeval: A benchmark and a toolkit for evaluating medical vision-language models. *arXiv preprint arXiv:2402.09262*, 2024.

Thrush, T., Jiang, R., Bartolo, M., Singh, A., Williams, A., Kiela, D., and Ross, C. Winoground: Probing vision and language models for visio-linguistic compositionality. In *Proceedings of the IEEE/CVF Conference on Computer Vision and Pattern Recognition*, pp. 5238–5248, 2022.

Tong, S., Jones, E., and Steinhardt, J. Mass-producing failures of multimodal systems with language models. *Advances in Neural Information Processing Systems*, 36, 2024a.

Tong, S., Liu, Z., Zhai, Y., Ma, Y., LeCun, Y., and Xie, S. Eyes wide shut? exploring the visual shortcomings of multimodal llms. In *Proceedings of the IEEE/CVF Conference on Computer Vision and Pattern Recognition*, pp. 9568–9578, 2024b.

Wang, J., Wu, Z., Li, Y., Jiang, H., Shu, P., Shi, E., Hu, H., Ma, C., Liu, Y., Wang, X., et al. Large language models for robotics: Opportunities, challenges, and perspectives. *arXiv preprint arXiv:2401.04334*, 2024a.

Wang, W., Su, Y., Huan, J., Liu, J., Chen, W., Zhang, Y., Li, C.-Y., Chang, K.-J., Xin, X., Shen, L., et al. Asclepius: A spectrum evaluation benchmark for medical multi-modal large language models. *arXiv preprint arXiv:2402.11217*, 2024b.

Wu, C., Lei, J., Zheng, Q., Zhao, W., Lin, W., Zhang, X., Zhou, X., Zhao, Z., Zhang, Y., Wang, Y., et al. Can gpt-4v (ision) serve medical applications? case studies on gpt-4v for multimodal medical diagnosis. *arXiv preprint arXiv:2310.09909*, 2023a.

Wu, C., Zhang, X., Zhang, Y., Wang, Y., and Xie, W. Towards generalist foundation model for radiology. *arXiv preprint arXiv:2308.02463*, 2023b.

Wu, M., Ji, J., Huang, O., Li, J., Wu, Y., Sun, X., and Ji, R. Evaluating and analyzing relationship hallucinations in lvlms. *arXiv preprint arXiv:2406.16449*, 2024.

Xia, P., Chen, Z., Tian, J., Gong, Y., Hou, R., Xu, Y., Wu, Z., Fan, Z., Zhou, Y., Zhu, K., et al. Cares: A comprehensive benchmark of trustworthiness in medical vision language models. *arXiv preprint arXiv:2406.06007*, 2024.

Xu, P., Shao, W., Zhang, K., Gao, P., Liu, S., Lei, M., Meng, F., Huang, S., Qiao, Y., and Luo, P. Lvlm-ehub: A comprehensive evaluation benchmark for large vision-language models. *arXiv preprint arXiv:2306.09265*, 2023.

Yuksekgonul, M., Bianchi, F., Kalluri, P., Jurafsky, D., and Zou, J. When and why vision-language models behave like bags-of-words, and what to do about it? *arXiv preprint arXiv:2210.01936*, 2022.

Zhang, S., Xu, Y., Usuyama, N., Bagga, J., Tinn, R., Preston, S., Rao, R., Wei, M., Valluri, N., Wong, C., et al. Large-scale domain-specific pretraining for biomedical vision-language processing. *arXiv preprint arXiv:2303.00915*, 2(3):6, 2023a.

Zhang, S., Xu, Y., Usuyama, N., Xu, H., Bagga, J., Tinn, R., Preston, S., Rao, R., Wei, M., Valluri, N., et al. Biomedclip: a multimodal biomedical foundation model pretrained from fifteen million scientific image-text pairs. *arXiv preprint arXiv:2303.00915*, 2023b.

Zhang, X., Wu, C., Zhao, Z., Lin, W., Zhang, Y., Wang, Y., and Xie, W. Pmc-vqa: Visual instruction tuning for medical visual question answering. *arXiv preprint arXiv:2305.10415*, 2023c.

Appendix

A Prompts for dataset curation

In this section, we provide the prompts used to interact with GPT-4o for dataset generation and MLLM evaluation. Wherever we use **TEXT**, we mean that TEXT is a description or variable that is image/pair specific.

A.1 Question generation

We use the following prompt to generate a question for a single confusing pair. We describe the output format as detailed as possible to be able to process the answers with little human interaction.

System message: You are a helpful assistant expert in the medical domain.
Prompt: Here is the description of two medical images that I can see:
Image1: **CAPTION OF IMAGE 1**
Image2: **CAPTION OF IMAGE 2**
Your task is to create multiple-choice questions. Follow the rules below.
1. The question should be about a property that is clearly visible in the images.
2. It should be possible to answer the question by only looking at the images.
3. Pretend that you can only see one image. You are not allowed to refer to 'Image1', 'Image2' or 'images'. You should also not create questions that require comparing the two images.
4. There should be exactly two answer options. You have to come up with a question for which the answer is different for the two images.
5. The answer options should be clearly different.
Please provide the question and the two answer options in the following format:
Question: <YOUR QUESTION>
Option1: <ANSWER 1>
Option2: <ANSWER 2>
Also, please provide the correct answers to the question for the images corresponding to our captions in the following format:
Image1: <ANSWER>
Image2: <ANSWER>
Aim for simple, efficient and concise questions to best test someone's knowledge and understanding of the underlying concepts.

A.2 Categorizing images

To categorize the images, we first show GPT-4o captions of several (here we use 100) images and ask it to separate them into different categories. Afterward, for each image, we ask GPT-4o to pick one of the categories for that image based on its caption.
We used the following prompt to extract categories:

System message: You are a helpful assistant expert in the medical domain.
Prompt: I have several medical images related to radiology that each one has a corresponding caption. I have listed the captions below. Can you go through the captions and categorize them? Please focus on the general categories.
Caption 0: **IMAGE 0 CAPTION**
Caption 1: **IMAGE 1 CAPTION**
...
Caption 99: **IMAGE 99 CAPTION**

Using this prompt, we find 9 categories: Cerebral, Spinal, Cardiac, Gastrointestinal, Musculoskeletal, Vascular, Pulmonary, Head and Neck, Breast, and Other.
We used the following prompt to assign categories:

System message: You are a helpful assistant expert in the medical domain.
Prompt: Caption: **IMAGE CAPTION**
The above caption describes a radiology image. To which of the following categories does this image belong? You should only name the category, and you do not need to specify your reasoning.
Categories: Cerebral, Spinal, Cardiac, Gastrointestinal, Musculoskeletal, Vascular, Pulmonary, Head and Neck, Breast, Other"

The final set of categories in our dataset are somewhat different, as we incorporated feedback from the radiologist to revise the automatically generated categories.

A.3 Finding failure modes

To find common failure modes that our dataset probes, we use the questions and captions of 100 pairs in the following prompt to send to GPT-4o:

System message: You are a helpful assistant expert in the medical domain.
Prompt: I am analyzing an image embedding model. I have several image pairs that each one has a corresponding two choice question. I know that the embedding model confuses the images about the corresponding question. Can you go through the questions, options, and image descriptions, trying to figure out some general patterns that the embedding model struggles with? Please focus on the visual features and generalize patterns that are important to vision models.
Pair 0
First image description: **IMAGE 1 CAPTION**
Second image description: **IMAGE 2 CAPTION**
Confusing multiple choice question: **QUESTION**
Pair 1
First image description: **IMAGE 1 CAPTION**
Second image description: **IMAGE 2 CAPTION**
Confusing multiple choice question: **QUESTION**
...
Pair 99
First image description: **IMAGE 1 CAPTION**
Second image description: **IMAGE 2 CAPTION**
Confusing multiple choice question: **QUESTION**

A.4 Free Form Evaluation

For the free-form (FF) GPT-4o evaluation, we pass the MLLM's answers with the following prompt to GPT-4o to obtain two scores, one for each answer option.

System message: `You are a helpful and precise assistant for checking the quality of the answer.`
Prompt: `[Question]`
`**QUESTION**`
`[Answer A]`
`**OPTION A**`

`[Answer B]`
`**OPTION B**`

`[Assistant]`
`**RESPONSE**`

`[End of Assistant]`

`[System]`
`We would like to request your feedback on the performance of an AI`
`assistant in response to the user question displayed above.  The user asks`
`the question on observing an image.  We have provided two possible answers,`
`[Answer A] and [Answer B] to the question.  Your job is to evaluate how`
`close the AI assistant's answer is to each of the answers.  You don't have`
`to decide whether the answers are correct or not.  Each answer should`
`receive an overall score on a scale of 1 to 10, where a higher score`
`indicates the AI assistant's answer is closer to the specific answer.`
`After providing the scores, concisely provide your explanation for the`
`given scores.  Remember, you don't need to comment on the correctness of`
`the answers.  Please provide your answer in the following format:`
`A: <SCORE>`
`B: <SCORE>`
`Your explanation:  <EXPLANATION>`

These scores are the similarities of the MLLM's answer to the different answer options. If the gap between the higher and lower score is at least 3, we assign the option with the higher score as the MLLM's output. Otherwise, we mark the answer as invalid.

B   Model details

In this section, we provide details on the versions and hyperparameters of MLLMs that we use. It should be noted that for the multiple choice (MC) evaluation mode, we set temperature to 0, as we only expect a single letter option to be generated.

MLLM	Version/LLM	Temperature	Beams	Top p
LLaVA	v1.6/Mistral 7B	0.2	1	-
BLIP-2	Opt 2.7B	1	5	0.9
InstructBLIP	Vicuna 7B	1	5	0.9
LLaVA-Med	v1.5/Mistral 7B	0.2	1	-
RadFM	-	-	-	-
Med-Flamingo	-	1	5	0.9
GPT	4o (release 20240513)	0.7	-	-
Claude	3 Opus	0.2	-	-
Gemini	1.5 Pro	0.2	-	-

Table 2: MLLM details

B.1   MedFlamingo few-shot prompting

In order for MedFlamingo to produce valid responses, we need to use few-shot prompting. Here, we show three questions and answers from PMC-VQA benchmarks Zhang et al. (2023c). The following is the prompt we used for MC evaluation:

```
Prompt:    You are a helpful medical assistant.  You are being provided with
images, a two choice question about each image and an answer.  Follow the
examples and answer the last question.  <image>Question:  What radiological
technique was used to confirm the diagnosis?
A: CT Scan
B: Mammography
Answer:  B: Mammography<|endofchunk|><image>Question:  What did the CT scan
show?
A: Cerebral edema
B: Intracranial hemorrhage
Answer:  A: Cerebral edema|endofchunk|><image>Question:  What is the
purpose of the asterisk shown in the figure?
A: To indicate the formation of lobes around the contracting nucleus.
B: To indicate the normal lentoid shape of hypocotyl nuclei.
Answer:  B: To indicate the normal lentoid shape of hypocotyl
nuclei.<|endofchunk|><image>
Question:  **QUESTION**
A: **OPTION A**
B: **OPTION B**
Answer:
```

The following is the prompt we used for FF evaluation:

```
Prompt:         You are a helpful medical assistant.  You are being provided
with images, a question about each image and an answer.  Follow
the examples and answer the last question.  <image>Question:  What
radiological technique was used to confirm the diagnosis?  Answer:
Mammography<|endofchunk|><image>Question:  What did the CT scan show?
Answer:  Cerebral edema|endofchunk|><image>Question:  What is the
purpose of the asterisk shown in the figure?  Answer:  To indicate the
normal lentoid shape of hypocotyl nuclei.<|endofchunk|><image>Question:
**QUESTION** Answer:
```

The following is the prompt we used for GD evaluation:

Prompt: You are a helpful medical assistant. You are being provided with images, a two choice question about each image and an answer. Follow the examples and answer the last question. <image>Question: What radiological technique was used to confirm the diagnosis?
A: CT Scan
B: Mammography
Answer: B: Mammography<|endofchunk|><image>Question: What did the CT scan show?
A: Cerebral edema
B: Intracranial hemorrhage
Answer: A: Cerebral edema|endofchunk|><image>Question: What is the purpose of the asterisk shown in the figure?
A: To indicate the formation of lobes around the contracting nucleus.
B: To indicate the normal lentoid shape of hypocotyl nuclei.
Answer: B: To indicate the normal lentoid shape of hypocotyl nuclei.<|endofchunk|><image>
Question: **QUESTION**
A: **OPTION A**
B: **OPTION B**
Answer:

The following is the prompt we used for PS evaluation:

Prompt: You are a helpful medical assistant. You are being provided with images, a question about each image and an answer. Follow the examples and answer the last question. <image>Question: What radiological technique was used to confirm the diagnosis? Answer: Mammography<|endofchunk|><image>Question: What did the CT scan show? Answer: Cerebral edema<|endofchunk|><image>Question: What is the purpose of the asterisk shown in the figure? Answer: To indicate the normal lentoid shape of hypocotyl nuclei.<|endofchunk|><image>Question: **QUESTION** Answer: **ANSWER**

C Examples and further results

Figure 4: Sample VQA from MediConfusion where the solution is directly provided in the image in the form of text and visual prompts (arrows). Medical MLLMs not trained for OCR have been unable to leverage the hint.
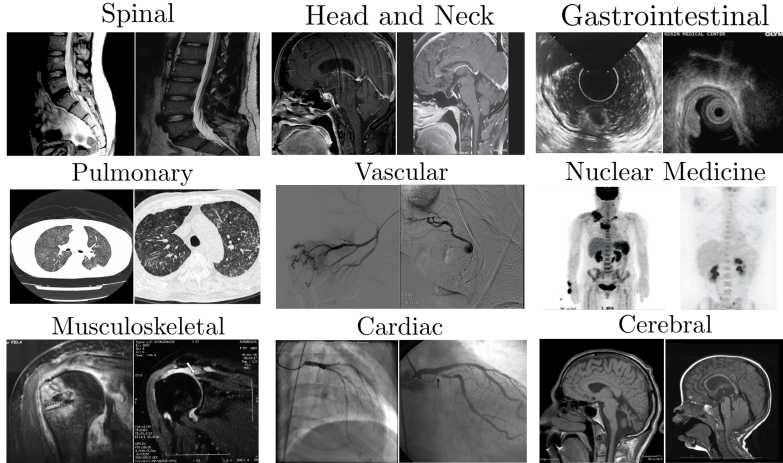
Figure 5: Sample confusing image pairs we have extracted from the ROCO dataset across 9 categories.

	Cerebral		Vascular		Head & Neck		Spinal		Musculoskel.		Cardiac		Gastroint.		Pulmonary		Nuclear Med.	
Model	Set	Indiv.	Set	Indiv.	Set	Indiv.	Set	Indiv.	Set	Indiv.	Set	Indiv.	Set	Indiv.	Set	Indiv.	Set	Indiv.
Llama 3.2	21.52	**60.76**	23.29	58.09	14.93	53.73	**19.61**	**64.71**	21.43	59.52	11.54	50.00	16.28	58.14	30.00	**65.00**	14.29	50.00
Molmo 72B	15.19	58.23	9.59	54.79	13.43	56.72	3.92	52.94	9.52	50.00	11.54	55.77	9.3	51.16	10.00	50.00	**28.57**	**64.29**
Molmo 7B	13.92	55.70	13.70	54.79	8.96	52.24	5.88	56.86	19.05	54.76	7.69	51.92	13.95	53.49	10.00	55.00	14.29	50.0
LLaVA	7.59	49.37	13.70	54.79	4.48	52.24	5.88	**52.94**	9.52	52.38	7.69	51.92	27.91	60.47	10.00	55.00	14.29	57.14
BLIP2	5.06	54.43	8.22	53.42	4.48	46.27	3.92	49.02	4.76	50.00	7.69	50.00	13.95	51.16	10.00	55.00	**28.57**	**64.29**
InstructBLIP	16.46	**59.49**	10.96	56.16	7.46	52.24	**17.65**	**52.94**	23.81	**59.52**	7.69	50.00	9.30	51.16	10.00	60.00	14.29	57.14
LLaVA-Med	1.27	53.16	2.74	49.32	0.00	50.75	0.00	50.98	4.76	50.00	0.00	50.00	4.65	53.49	0.00	45.00	0.00	50.00
RadFM	1.27	49.37	4.11	49.32	5.97	49.25	3.92	50.98	2.38	50.00	11.54	50.00	11.63	53.49	10.00	50.00	0.00	50.00
Med-Flamingo	7.59	58.23	10.95	56.16	8.96	52.24	0.00	52.94	4.76	52.38	3.85	51.92	2.33	48.84	10.00	50.00	0.00	50.00
GPT-4o	15.19	59.49	34.25	67.12	8.96	**58.21**	15.69	52.94	14.29	52.38	19.23	55.77	16.28	55.81	**35.00**	**65.00**	14.29	42.86
Claude 3 Opus	7.59	55.70	20.55	58.90	0.00	44.78	0.00	**52.94**	9.52	45.24	11.54	53.85	11.63	51.16	10.00	50.00	14.29	50.00
Gemini 1.5 Pro	**25.32**	58.23	27.40	60.27	**16.42**	52.24	**17.65**	43.14	**26.19**	47.62	7.69	48.08	23.26	44.19	5.00	50.00	**28.57**	57.14

Table 3: Results by category. We report the best set and individual accuracies (%) for each model across all evaluation techniques.